DOI: http://dx.doi.org/10.12989/sem.2010.36.4.401

Coupled thermal and structural analysis of roller compacted concrete arch dam by three-dimensional finite element method

Khaled H. Bayagoob[1a], Jamaloddin Noorzaei*[2], Aeid A. Abdulrazeg[1a], Awad A. Al-Karni[3] and Mohd Saleh Jaafar[1b]

[1]Civil Engineering Department, Universiti Putra Malaysia, 43400 UPM-Serdang, Malaysia
[2]Institute of Advance Technology, Universiti Putra Malaysia, 43400 UPM-Serdang, Malaysia
[3]Civil Engineering Department, King Saud University, Riyadh, Saudi Arabia

(Received July 5, 2009, Accepted December 21, 2009)

Abstract. This paper focuses on the development, verification and application of a three-dimensional nite element code for coupled thermal and structural analysis of roller compacted concrete arch dams. The Ostour Arch dam located on Ghezel-Ozan River, Iran, which was originally designed as conventional concrete arch dam, has been taken for the purpose of verication of the nite element code. In this project, RCC technology has been ascertained as an alternative method to reduce the cost of the project and make it competitive. The thermal analysis has been carried out taking into account the simulation of the sequence of construction, environmental temperature changes, and the wind speed. In addition, the variation of elastic modulus with time has been considered in this investigation using Concard's model. An attempt was made to compare the stresses developed in the dam body five years after the completion of the dam with those of end of the construction. It was seen that there is an increase in the tensile stresses after five years over stresses obtained immediately at the end of construction by 61.3%.

Keywords: arch RCC dam; thermal analysis; stress analysis; finite element modeling.

1. Introduction

The design and construction of roller compacted concrete dam (RCC) structures involves the problem of thermal stresses and temperature control. In RCC dams, the material temperature changes due to the hydration of cement and the environmental boundary conditions. When the temperature of a structure varies, there is a tendency to produce thermal stresses (Yuksel 2009). If these thermal stresses, in addition to the tensile stresses resulting from other loads such as gravity and hydrostatic load, exceed the tensile strength of RCC, crack will develop in the dam body.

Zhang *et al*. (1996) analyzed the stress distribution in arch RCC dam body to evaluate the stability of cracks by determining the stress state in RCC body weakened by multiple cracks under

*Corresponding author, Associate Professor, E-mail: jamal@eng.upm.edu.my
[a]PhD Candidate
[b]Professor

harmonic temperature variation. The result has shown that, the maximum tensile stresses occurred at the upstream surface of both abutments and the downstream reaches of the arch crown. However, the integral equation method used to calculate temperature and the stress distribution in the two dimensional domain, whereas the problem is a three dimensional problem. The effect of reservoir water temperature was neglected. In addition, this method was applied only for a small RCC arch dam in horizontal section.

Malla and Wieland (1999) proposed a three-dimensional finite element model of the dam-foundation system to investigate an arch-gravity dam with a horizontal crack. The thermal and elastic properties of a linear-elastic model were determined based on the available records of the concrete and air temperatures, and the dam displacements measured by means of a pendulum located in the central part of the dam. Computer program called ADINAT was used to perform the thermal analysis. It was concluded that the seasonal variation of the temperature distribution made the major contribution to the elastic part of the radial displacements of the dam.

Shuping *et al*. (1999) performed an emulation analysis of two RCC arch dams using three dimensional nonlinear finite elements. The first arch RCC dam named Puding and the second named Shapai which are all located in China. It has been found that, the thermal stresses are too high for the construction plan without contraction joints. However, the effect of dam foundation interaction was ignored.

Nilipour (2003) performed a thermal analysis for a concrete arch dam comparing roller compacted concrete (RCC) with convectional block construction method. The effect of method of construction is investigated using a commercials finite element software (Z_Soil 3D), taking into account concreting steps, it was concluded that, at the same elevation higher temperature rise is experienced in the core of the dam in applying conventional method as compared with RCC method. Based on the calculated maximum principal stresses it is revealed that higher tensile stress occurs in the model using conventional method in the early age of concrete. Whereas, maximum tensile stress in RCC model occurs later due to operation loads comparatively with a lower value, hence post-cooling is not necessary in RCC construction method.

Hongwei and Yaolong (2005) used a three-dimensional finite element relocating mesh method to simulate the temperature distribution for different pipe cooling scheme in RCC arch dam during construction and operation period. In their work many factors had also been considered, such as thermal adiabatic rise of temperature with age, the process of placement by layer, work suspension in summer and the change of air temperature. The results showed that the cooling effect was notable and the maximum temperature at the centre of the dam was effected by the layout range of pipe cooling. However, the structural response of the dam was not reported.

Sheibany and Ghaemian (2006) used a finite element method to investigate annual variation of temperature and thermal stress in the body of Karaj arch dam in Iran. In this study, appropriate heat transfer boundary conditions in the dam body have been used for air and reservoir temperature as well as solar radiation variations. The temperatures predicted by the proposed finite element model were satisfactorily compared with the instrumentation records measured at dam site. Finite element result has shown that, probable cracks occur in a very narrow region of the downstream face. Thermal loads have the most significant effects for causing downstream cracks in comparison with other loads which act on the dam body such as; self-weight and hydrostatic loads.

Lingfei and Li (2008) used a three-dimensional finite element model to simulate the whole process of temperature field and thermal creep stress of Xiaowan high arch dam during construction phase. In this investigation, thermal and mechanical properties, concrete construction, temperature variation of environment, crown filling and water impoundment orders have been considered. The finite element results have shown that, the maximum transverse directional thermal creep stress and downstream directional thermal creep stress are both less than the allowable horizontal tensile stress and temperature crack will not appear.

Zhang *et al*. (2009) developed a three-dimensiona finite element relocating mesh method based on the construction property of rolled compacted concrete arch dam to simulate construction process and compute temperature field. The results show that the method has high calculation precision, less computer run time and less memory. The values computed with the method are in the same trend with the observation data. However, the study was limited for thermal analysis only.

It is evident from the above literature review that, that there is little amount of research work have been carried out concerning the arch RCC dams. The only work of shuping (1999), Zhang (1996) and Zhang (2009) are directly related the pariticulart Arch RCC dam in conjunction to all the above shortcoming, the main objectives of present study are:

i. Develop Three Dimension Finite Element program to analyze arch RCC problem. This code has the capability to execute; a) Thermal analysis, b) Structural analysis, c) Coupled analysis.
ii. Thermal modeling include actual environmental temperature changes, and the wind speed which have been recorded at the project site.
iii. Develop special mesh generation code to model the arch RCC dam and simulate the progress of the dam construction.

In the framework of the present study, an initial analysis of the heat generation and dissipation in the dam was conducted. Later, structural analysis of the dam was carried out by converting the change temperature into equivalent nodal forces in addition to dead weight of the dam and hydrostatic force. The finite element formulation based on the Galerkin approach was adopted to evaluate the temperature distribution.

2. Computation of unsteady thermal field

The general partial differential equation governing heat flow in a three-dimensional solid medium is expressed as, Incropera and DeWitt (2002)

$$\frac{\partial}{\partial x}\left(k_x\frac{\partial T}{\partial x}\right)+\frac{\partial}{\partial y}\left(k_y\frac{\partial T}{\partial y}\right)+\frac{\partial}{\partial z}\left(k_z\frac{\partial T}{\partial z}\right)+\dot{Q} = \rho c\frac{\partial T}{\partial t} \tag{1}$$

where T is the solid temperature (°C); k_x, k_y, and k_z are the concrete conductivity coefficients in x, y and z directions, respectively, (W/m °C); $\dot{Q}$ is the rate of the heat introduced per volume (W/m^3); ρ is the material density (kg/m^3), and; c is the solid specific heat (J/kg °C).

The following boundary conditions govern the temperature change in three dimensional, Sergerlind (1984)

$$T = T_p \tag{2a}$$

$$k_x\frac{\partial T}{\partial x}l_x+k_y\frac{\partial T}{\partial y}l_y+k_z\frac{\partial T}{\partial z}l_z+q+h(T_s-T_f) = 0 \tag{2b}$$

where T_p is the known values of the nodal temperatures on the boundaries; q is flowing heat from surface; h is the film coefficient; T_s is unknown temperatures at the boundary nodal points; T_f is the ambient temperature; l_x, l_y and l_z are the direction cosines of the outward normal to the surface under consideration.

3. Finite element simulation

The finite element method was used as solution scheme in this study based on the Taylor-Galerkin approach. Upon applying this approach, the following system of differential equations is obtained

$$[K]^{(e)}\{T\}^{(e)} - [C]\{\dot{T}\}^{(e)} = \{F\}^{(e)} \tag{3}$$

The finite difference approximation was used for solving Eq. (3) in the time domain numerically. This solution (after assembly of the stiffness matrices) is given by Noorzaei *et al*. (2006)

$$([C] + \theta\Delta t[K_t])\{T\}_b = ([C] + \theta\Delta t[K_t])\{T\}_a + \Delta t((1-\theta)\{F_t\}_a + \theta\{F_t\}_b) \tag{4}$$

where $\{T\}_b$ and $\{F_t\}_b$ are $\{T\}$ and $\{F_t\}$ at time (b) and $\{T\}_a$ and $\{F_t\}_a$ are $\{T\}$ and $\{F_t\}$ at time (a), θ is a scalar ($0 \le \theta \le 1$) which is equal to 2/3 in Galerkin method. Then Eq. (6) takes the following general form

$$[A_G^*]\{\Delta T\} = \{F_G^*\} \tag{5}$$

where

$$[A_G^*] = \frac{1}{\Delta t}[C] + \frac{2}{3}[K_t] \tag{6}$$

$$\{F_G^*\} = \frac{1}{2}(\{F_t\}_a + 2\{F_t\}_b - 3[K_t]\{T\}_a) \tag{7}$$

where $\{\Delta T\}$ represents the temperature changes at the nodal points with respect to increment time Δt which is used for evaluation of temperatures at the new time stage using the following expression

$$\{T\}_{(b)} = \{T\}_{(a)} + \frac{2}{3}\{\Delta T\} \tag{8}$$

Since conductivity coefficient (k_x, k_y, k_z), density (ρ), specific heat (c) are constants, the value of the $[C]$ and $[K]$ in the above expressions are also constant over each element. Hence the matrix $[A_G^*]$ for each element has a constant value for each time interval. Therefore, the nodal temperature changes are only based on the value of the heat load vector ($\{F_G^*\}$). In other words the temperatures variations with time will depend only on the values of concrete hydration rate (Q') and the ambient temperature (T_f).

4. Computational strategies for thermal analysis

The computational steps adopted for thermal analysis during construction phase are summarized as:

i) Take the first stage and divide the construction time into several time increments (optimum time step in terms of hours)

ii) Evaluate the matrices [C] and [K], $[A_G]$ and its inverse.

iii) Calculate the load vector $\{F_G\}$ using Eq. (7) and solve Eq. (5) to evaluate the changes of temperatures $\{\Delta T\}$.

iv) $\{\Delta T\}$ has been added to the initial *RCC* temperature vector using Eq. (8). It should be noted that, the temperature vector $\{T\}_i$ of the ith time increment Δt_i will be the initial temperature vector for the next time increment Δt_{i+1}.

v) Repeat the steps iii to iv until the construction of the first stage is completed.

vi) Take the next stage in addition to the previous stage and repeat steps ii to iv until the final stage of construction. The flow chart of the above computational steps is presented in Fig. 1.

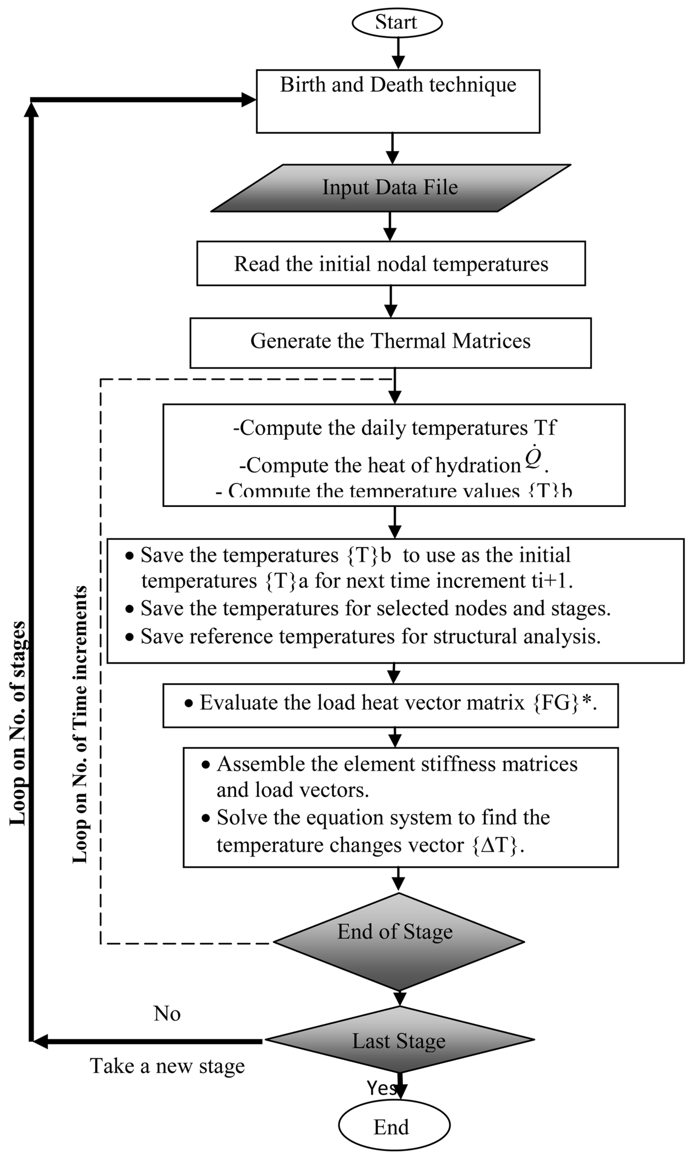

Fig. 1 Finite element code for thermal analysis

5. Stress analysis

The structure will be divided into stages according to construction schedule. Thus, the geometry and gravity loads of mass concrete structures can be updated during construction stages. Each stage will be discretized into elements, describes the stress-strain behavior of each element according to its constitutive relationship, then it assembles the elements at nodes. The general procedure followed in the stress analysis are shown in Fig. 2

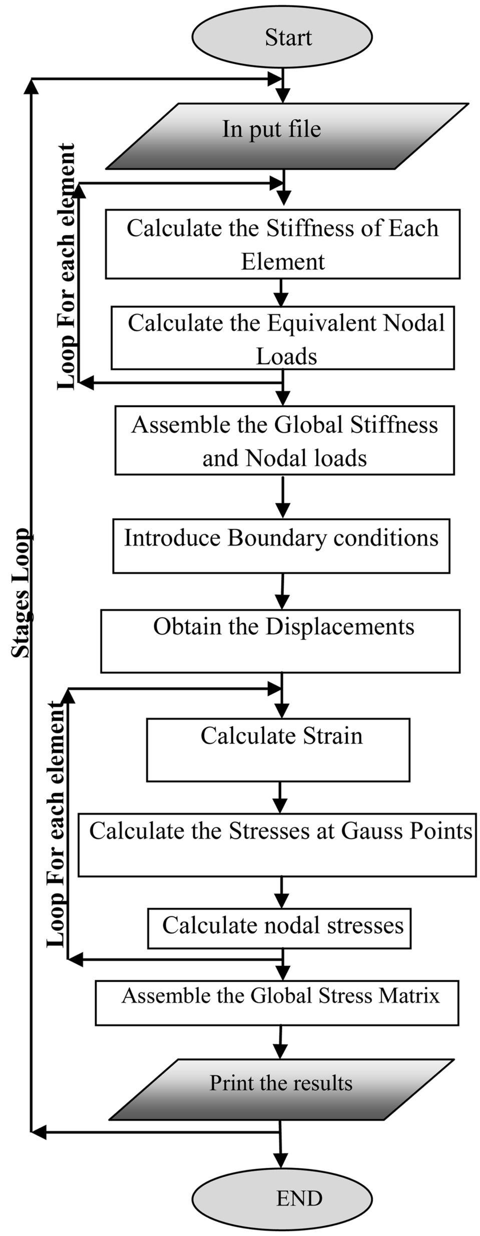

Fig. 2 Finite element code stress analysis flow chart

6. Coupled analyses

The structural analysis is preformed after the execution of the thermal analysis, one of the most important factors is that the elastic modulus of concrete increases with time. In this study the model which was developed by Concard *et al*. (2003) who had investigates the variation of RCC elastic model with time as expressed Eq. (9). This module was chosen in this study for generating the equivalent nodal force due to initial strains caused by temperature and stiffness matrix for each element. An outline of this algorithm for linear analysis is presented in Fig. 3

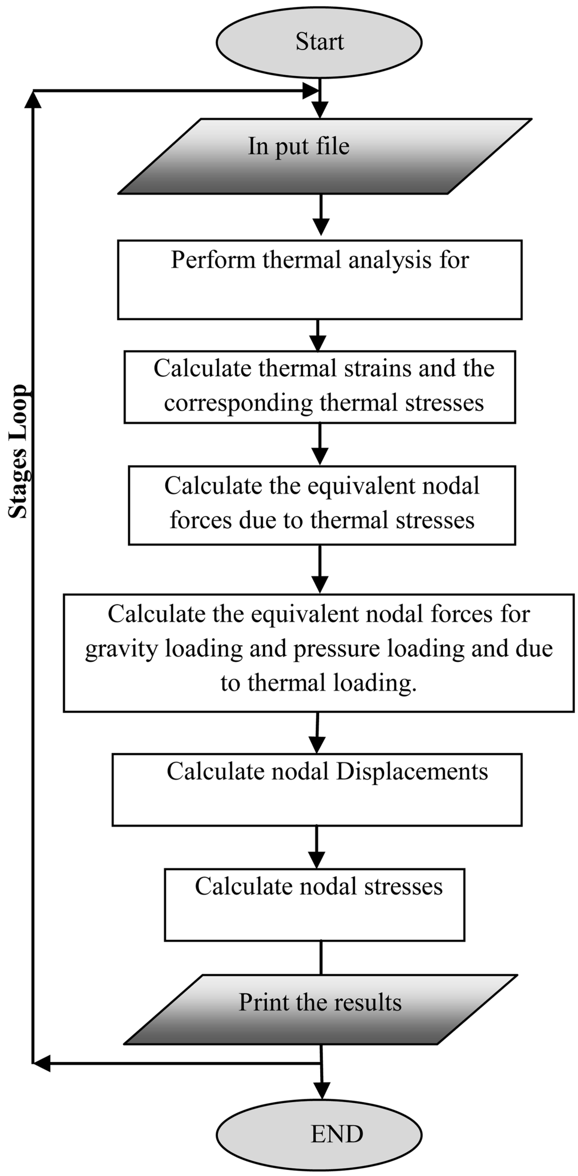

Fig. 3 Flow chart for coupled analysis

$$E_c(t) = E_c e^{at^b} \tag{9}$$

where $E_c(t)$ is the time dependent modulus in MPa, E_c is the final elastic modulus, t is the concrete age in days, and a and b are the model parameters which are taken as $a = -0.5$ and $b = -0.63$.

7. Development of the finite element code

7.1 Mesh generation finite element program (arch dam –Foundation- bodies system)

The problem of RCC arch dam idealization greatly differs from that of normal concrete arch. The normal concrete arch dam are usually constructed from individually concrete blocks (cantilevers), while the RCC arch dams are constructed from RCC layers which are placed layer by layer starting from dam bottom. A computer code was developed by the earthquake engineering research center in university of California for idealization of concrete arch dam problem (ADAP), Ghanaat *et al.* (1989). The ADAP code idealization will be not applicable for RCC arch dams. Thus in this study, this code has been extensively modified according to the RCC arch dams construction sequence.

In the modification version the ADAP which is specifically written for arch RCC dams the element and node numbering of the dam body is started from the bottom in order to simulate the progress of the dam construction.

7.2 Finite element analysis code

The three finite element software developed by Noorzaei *et al.* (2005) have been significantly modified to incorporate the followings:

a) Thermal analysis which is presented in sections 3 and 4.

b) Structural analysis discussed in section 5

The developed finite element program is written in Fortran language and can work under power station environment, Bayagoob (2008). The developed finite element program has the capability to execute each analysis individually or combined them as couple that is thermal and structural analysis simultaneously analysis), for this purpose a predefined index has been fixed at the beginning of the program where;

NTYPA=1 for thermal analysis, *NTYPA*=2 for structural analysis, and *NTYPA*=3 for coupled analysis.

8. Validation test

The primary objectives of the present study is to analyze a double curvature arch *RCC* dam, hence a curved cantilever beam shown in Figs. 4(a)-(b) has been chosen under the following two load cases:

i. Thermal load of 50ºC acts on the outer surface of the beam.

ii. Point load of 10 kN at the free end in the negative X direction

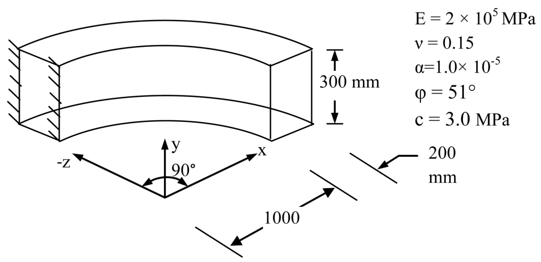

Fig. 4(a) Curved cantilever beam and material properties

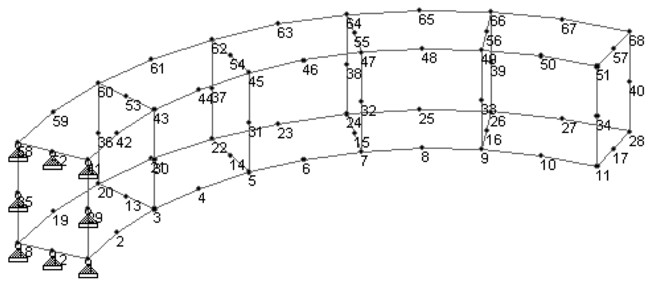

Fig. 4(b) Discretization of the curved cantilever beam

Case-i) Thermal load of 50ºC acts on the outer surface of the beam.

In order to verify the developed code for the analysis of structures subjected to thermal loads, the outer surface of the curved beam is assumed to heat up by a temperature of 50ºC. The finite element analysis results for the deflection along the outer radius are compared with the result obtained using the Lusas software Fig. 5 shows the comparison.

Case-ii) Point load of 10 kN at the free end in the negative x direction

A point load 10 kN is assumed to be acting on the free end in the negative X direction. The obtained result was compared with that obtained using the Lusas software. The comparison was made between the deflections along the outer radius as shown in Fig. 6. It is clear that the obtained results are in good agreement with those of the Lusas software.

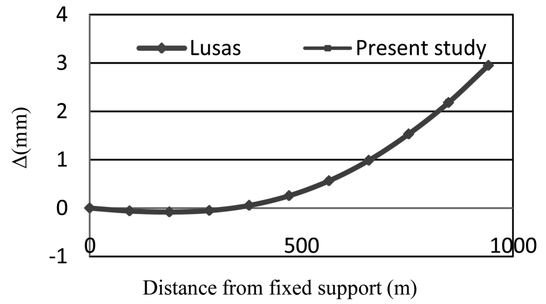

Fig. 5 Comparison of displacements along the upper outer radius (mm) for thermal loading

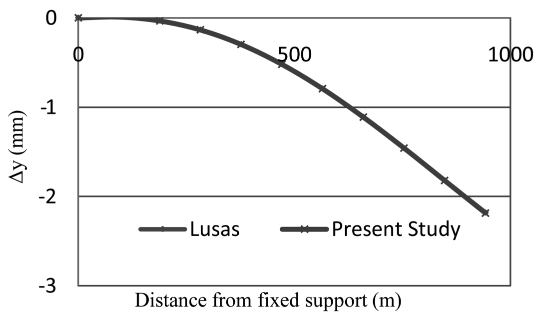

Fig. 6 Comparison of displacements along the upper outer radius (mm) for linear analysis

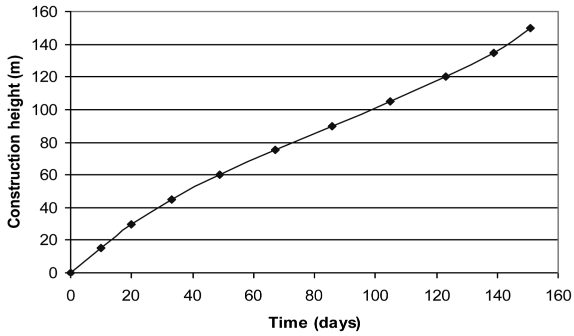

Fig. 7 Ostour dam construction schedule

minimum of the range of 0.19 to 0.29 for the recent constructed RCC arch dams, Qiuhua (2003). However, the valley with unsymmetrical shape can be considered as a narrow valley because the crest length to height ratio (L_c/H) is smaller than 4, U.S. Army Corps of Engineers (1987). Hence double curvature arch RCC dam is the suitable type of Arch dam for this particular gorge.

9.1 Construction schedule

The construction schedule of the dam is made up by considering the geometry of the dam and the site climatic conditions. To avoid the provision of the contraction joints which are forms the planes of weakness of the dam, it is necessary to complete the dam construction in one winter. From the geometry of the dam body, the *RCC* total volume required is 360,000 m^3, so with an average daily concreting capacity of 3500 m^3 and the *RCC* placing operation of 24 hour non-stop 5 days a week. This assumption leads to 103 working days or 21 weeks, so starting the dam construction in 1st of December 2003 and completing in the end of April, it is possible to construct the dam in one winter season. The progress of the dam construction with respect to time is illustrated in Fig. 7.

9.2 Material properties and site conditions

The material properties for the RCC, and the rock foundation are summarised in Table 1. The cementitious content of the RCC mix was taken as 100 kg/m^3 Ordinary Portland Cement and 100 kg/m^3 Fly Ash. These values were chosen based on average values reported in the literature. The average monthly temperature variation from 1990 to 2003 used in the analysis which was taken as those recorded in Mianeh city which located 36 km from the project site is shown in Fig. 8. The Civil engineering structures are subjected to varying environmental and operational conditions such as wind, temperature, and solar radiation (Zhou *et al*. 2008). Thus in the present study, The effect of solar radiation during the construction was incorporated by allowing an increase in ambient temperature of 1.0ºC to account for solar radiation heating of the concrete surface (ACI 207, 2004).

The surface heat transfer coefficient h (Eq. (10)) is applied to all exposed surfaces to simulate the convection heat transfer effect between the surrounding air and concrete surface. This convection coefficient is calculated using equation (100 taking into account the average annual wind speed which is 1.8 m/s recorded for 14 years (1990-2003) at Mianeh city which is close to the project site.

Table 1 Material properties for ostour arch dam

Material properties	Materials	
	Rock ground	RCC
Heat conduction coeff. k (W/m)	2.97	2.7
Heat convection coeff. h (W/m^2)	12.7	12.7
Specific heat c (kJ/kg·^{o}C)	1.0	1.15
Material density ρ (kg/m^3)	2600	2325
Elasticity modulus E (MPa)	18200	24000
Poisson ratio (ν)	0.2	0.2

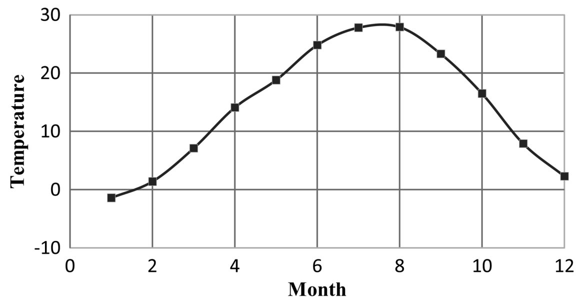

Fig. 8 Annual and average recorded monthly temperatures

$$h = h_c + h_w \tag{10}$$

where the average value of h_c is taken as h_c = 6.0 W/m^2 ^{o}C for concrete surface, and h_w is approximately related to the wind speed v as h_w = 3.7 v, (v in m/s). Thus using Eq. (10), yields h = 12.6 W/m^2 ^{o}C.

9.3 Finite element modeling

The 3D finite element mesh model of the deepest dam block is shown in Fig. 9. Twenty-node

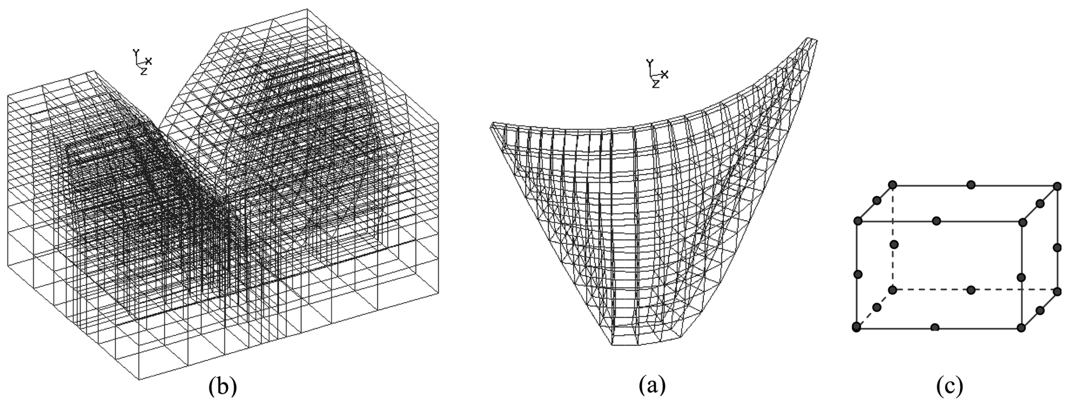

Fig. 9 Finite element modeling of the ostour dam (a) Dam-foundation system, (b) Dam body, (c) Twenty-node isoparametric elements

isoparametric elements are used in the analysis. The mesh of the dam body was generated using the developed mesh generation code.

10. Simulation of the initial conditions

The temperature distribution in the rock foundation and the RCC placing temperature are the two initial conditions considered in the analysis, Jaafar *et al*. (2004).

10.1 Evaluation of the initial foundation temperature

The determination of the foundation initial temperature is usually performed by the thermal analysis of the block foundation for a period of two or three years prior to the dam construction time, Ishakawa (1991).

In this case of study, the main annual temperature recorded near the project site is 14.2ºC. So this value is assigned first to the all nodes of the block foundation as an initial condition. Then heat transfer between the atmospheric temperature and the block foundation is performed for a period of two years using the average monthly temperature in Fig. 8.

10.2 RCC placement temperature

The RCC placement temperature was taken as that of the air temperature at the placing time of every RCC lift but not allowed to drop below 10ºC to account for the additive of mixing and the transportation of the fresh RCC, Noorzaei *et al*. (2006).

11. Results and discussion

The thermal analysis of Ostour arch RCC dam has been performed for the following stages:

i. End of construction
ii. Five years after the end of construction.

11.1 Thermal response

The initial temperature of the rock foundation block was evaluated using the technique on the section 10.1. Fig. 10 shows the isothermal contours for thermal analysis result of the block foundation for the two years period. It was observed that, only a layer of 30 m deep is affected by the environmental temperature changes.

After that, the thermal analysis for the dam body was executed using the construction schedule presented in Fig. 7 and the average monthly environmental temperature (1st of December up to the end of end of April) shown in Fig. 8.

Figs. 11 and 12 show the isothermal contours obtained immediately after the end of construction and after five years of the dam construction respectively. The maximum predicted temperatures after the end of construction and five years are 34 and 18ºC respectively. The minimum predicted temperatures after the end of construction and five years are 14 and 10.5ºC respectively. Due to

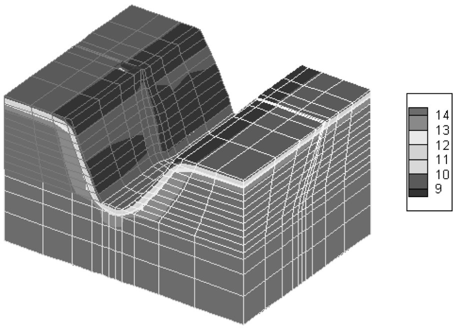

Fig. 10 Foundation block initial temperature distributions

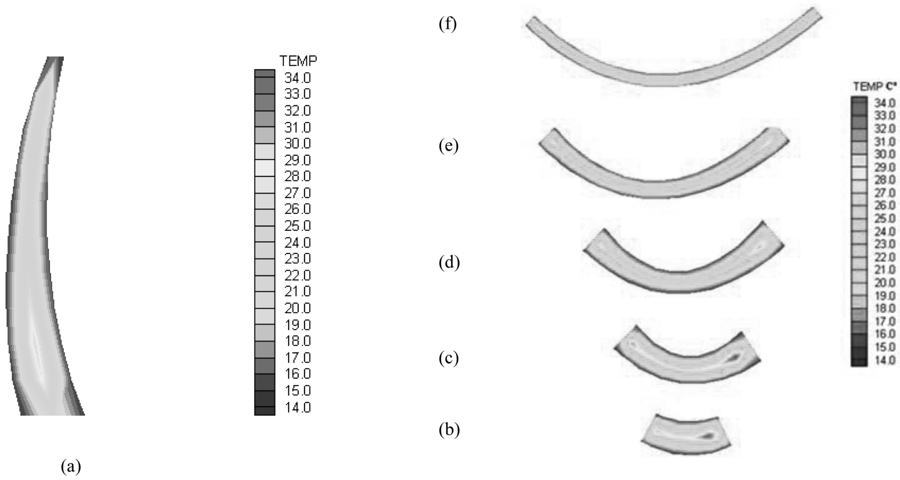

Fig. 11 Temperatures distribution through the crown cantilever and different elevation at the end of construction (a) Crown cantilever section, (b) Horizontal section at level = 15 m, (c) Horizontal section at level = 45 m, (d) Horizontal section at level = 75 m, (e) Horizontal section at level = 105 m, (f) Horizontal section at level = 135 m

equal predicted temperatures at the exposed boundaries of the dam body and the block foundation (14.0ºC), the temperature distributions within the dam body and the block foundation can't be presented clearly, for this reason, the thermal analysis results are plotted at different vertical and horizontal sections through the dam body as shown in Figs. 11 and 12 respectively.

Higher temperatures zones have been observed at the end of the dam construction especially at the lower elevation levels (15 m, 45 m, and 75 m) near the abutments as shown in Figs. 11(b)-(c). This can be anticipated due to the larger thicknesses at these locations which provide high insulating property compared to the upper levels where the dam thickness decreased progressively and also the exposed surface are more compare to the lower part. So the heat of hydration takes long time to dissipate to the surroundings at the lower elevation levels.

It is clearly observed that, the higher temperature zone still remaining at the lower levels, even after five years of exposing time to the environment. These zones are gradually decreased in size and contour levels values in the upward direction along the dam height Figs. 12(a)-(d). These zones

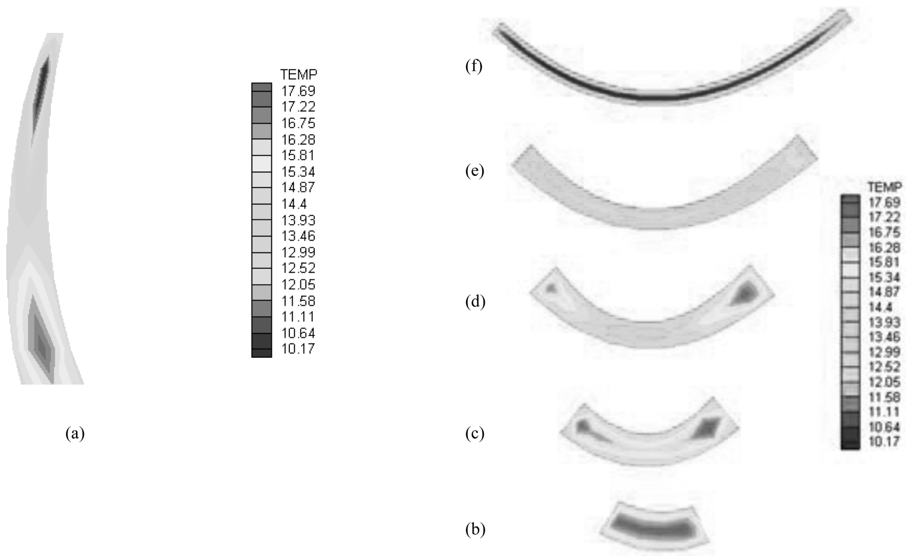

Fig. 12 Temperatures distribution through the crown cantilever and different elevation after five year after the end of construction (a) Crown cantilever section, (b) Horizontal section at level = 15 m, (c) Horizontal section at level = 45 m, (d) Horizontal section at level = 75 m, (e) Horizontal section at level = 105 m, (f) Horizontal section at level = 135 m

become lesser than the air temperature values in upper part of the dam body levels Figs. 12(e)-(f), this may be due to the complete dissipated heat of hydration at these locations and the gained heat energies from the previous cold months.

11.2 Structural response

To be compatible with thermal analysis, the structural analysis has been performed for the above two cases of the thermal analysis under the combination of the following load cases; (self weight, thermal loads, and hydrostatic pressure for the maximum overflow level of 150 m).

Fig. 13 show the principal stress distribution σ_1 (MPa), It is clearly observed from these plots, the presence of high tensile stresses at the dam bottom and the abutment boundaries Figs. 13(a)-(b). While compressive stresses contours are concentrated the dam body with high values at the lower levels of the upstream face which are gradually decreased in the direction of upper levels and the downstream. Generally, it is observed that most of the dam body under compressive stresses and tensile stresses has been observed at the toe Fig. 13(c) and the abutment boundaries, Figs. 13(a)-(b).

Similar plots are drawn for the intermediate principal stress σ_2 (MPa) as shown in Fig. 14. Tensile stresses of small values have been observed at the same locations of the principal stress σ_1. In addition, high compressive stresses zones are formed at some levels Figs. 14(c)-(f).

Fig. 15 shows the distribution of the minimum principal stress σ_3. High compressive stress zones concentric the upstream dam side which gradually decreased in the direction of abutment sides and the crest. In addition small regions of high compressive stresses have been observed near the abutment sides Figs. 15(e)-(f).

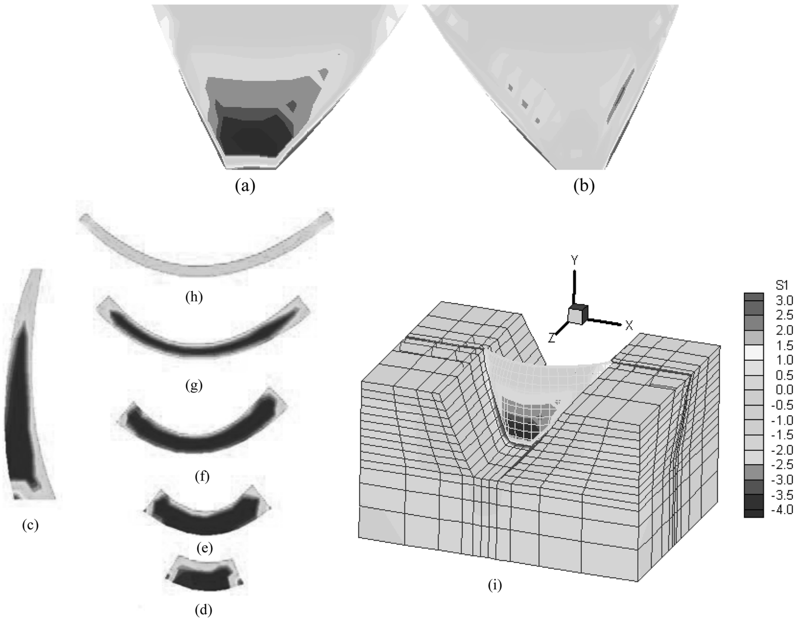

Fig. 13 Principal stress distribution (σ_1) at the end of dam construction (a) Upstream face, (b) Downstream face, (c) Crown cantilever section, (d) Horizontal section at level = 15 m, (e) Horizontal section at level = 45 m, (f) Horizontal section at level = 75 m, (g) Horizontal section at level = 105 m, (h) Horizontal section at level = 135 m, (i) Block foundation and the dam body

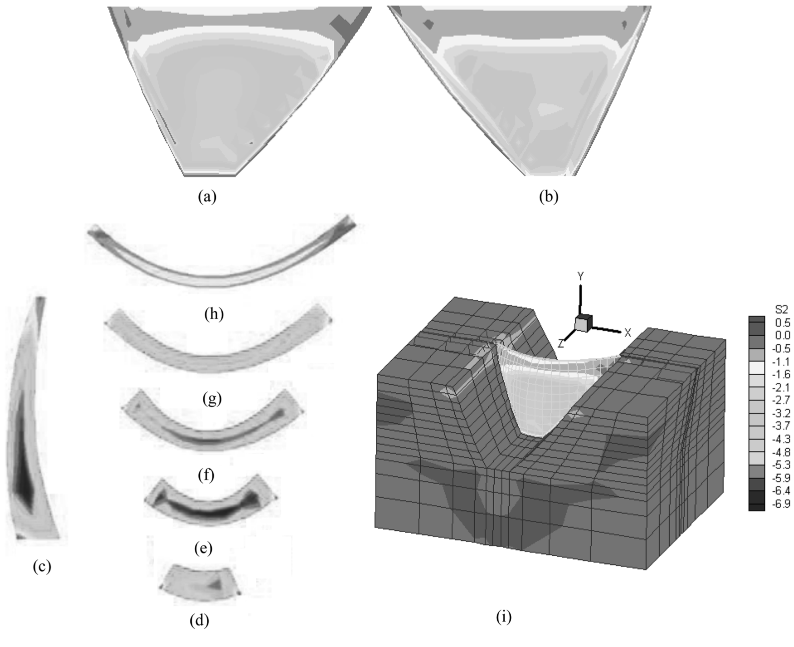

Fig. 14 Principal stress distribution (σ_2) at the end of dam construction (a) Upstream face, (b) Downstream face, (c) Crown cantilever section, (d) Horizontal section at level = 15 m, (e) Horizontal section at level = 45 m, (f) Horizontal section at level = 75 m, (g) Horizontal section at level = 105 m, (h) Horizontal section at level = 135 m, (i) Block foundation and the dam body

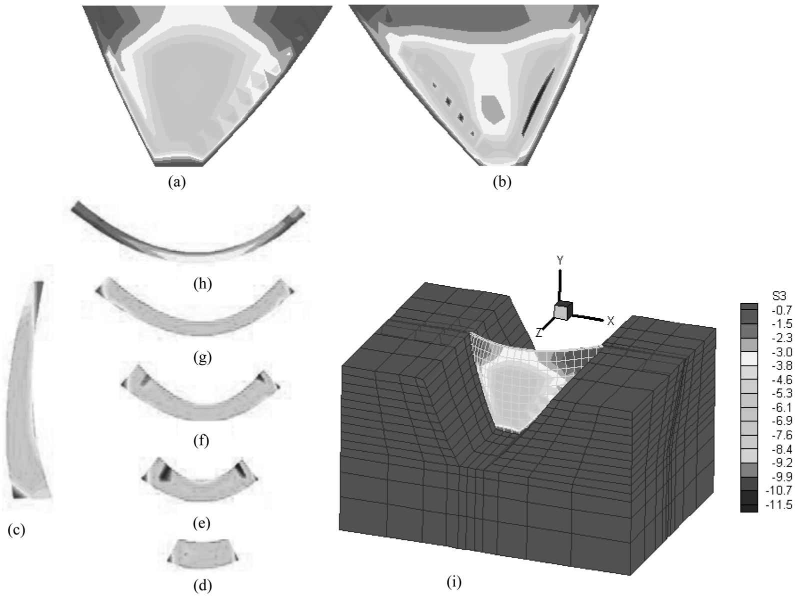

Fig. 15 Principal stress distribution (σ_3) at the end of dam construction (a) Upstream face, (b) Downstream face, (c) Crown cantilever section, (d) Horizontal section at level = 15 m, (e) Horizontal section at level = 45 m, (f) Horizontal section at level = 75 m, (g) Horizontal section at level = 105 m, (h) Horizontal section at level = 135 m, (i) Block foundation and the dam body

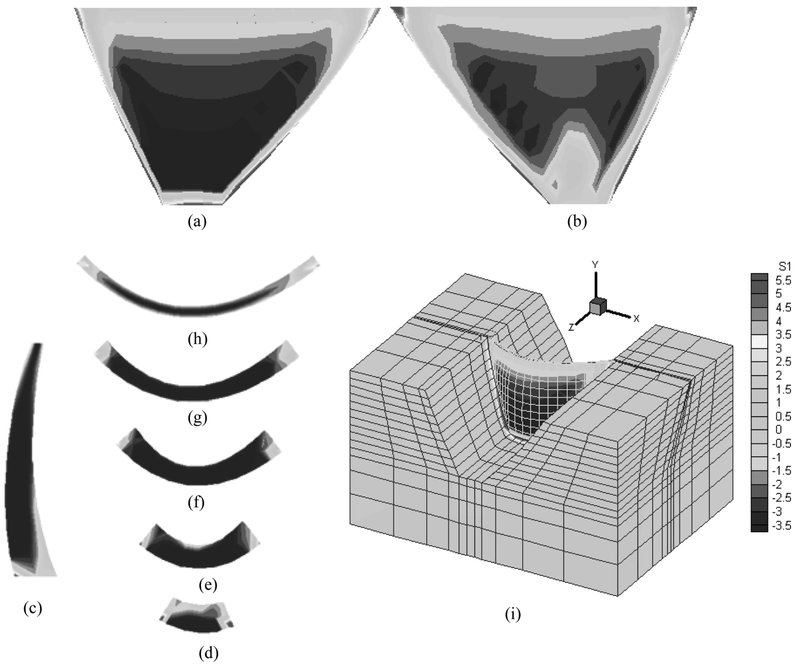

Fig. 16 Principal stress distribution (σ_1) after five years of the dam construction (a) Upstream face, (b) Downstream face, (c) Crown cantilever section, (d) Horizontal section at level = 15 m, (e) Horizontal section at level = 45 m, (f) Horizontal section at level = 75 m, (g) Horizontal section at level = 105 m, (h) Horizontal section at level = 135 m, (i) Block foundation and the dam body

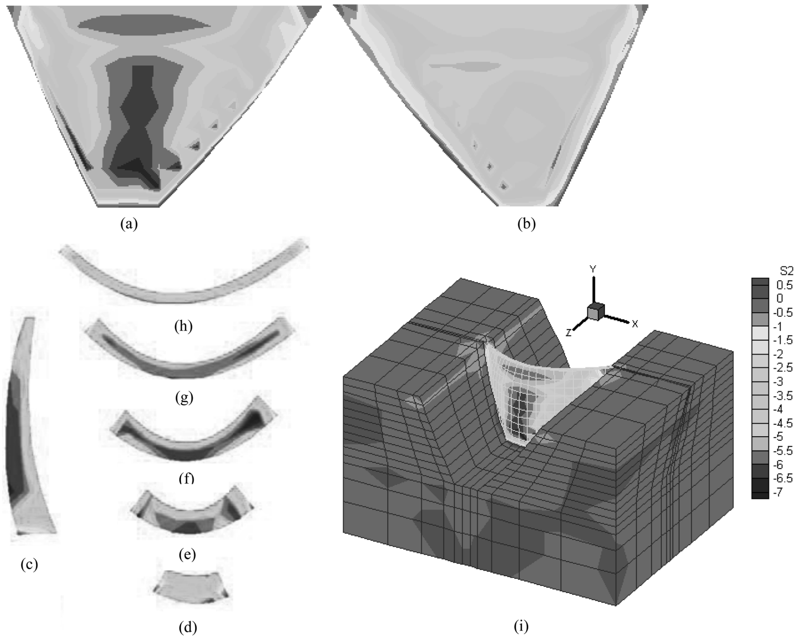

Fig. 17 Principal stress distribution (σ_2) after five years of the dam construction (a) Upstream face, (b) Downstream face, (c) Crown cantilever section, (d) Horizontal section at level = 15 m, (e) Horizontal section at level = 45 m, (f) Horizontal section at level = 75 m, (g) Horizontal section at level = 105 m, (h) Horizontal section at level = 135 m, (i) Block foundation and the dam body

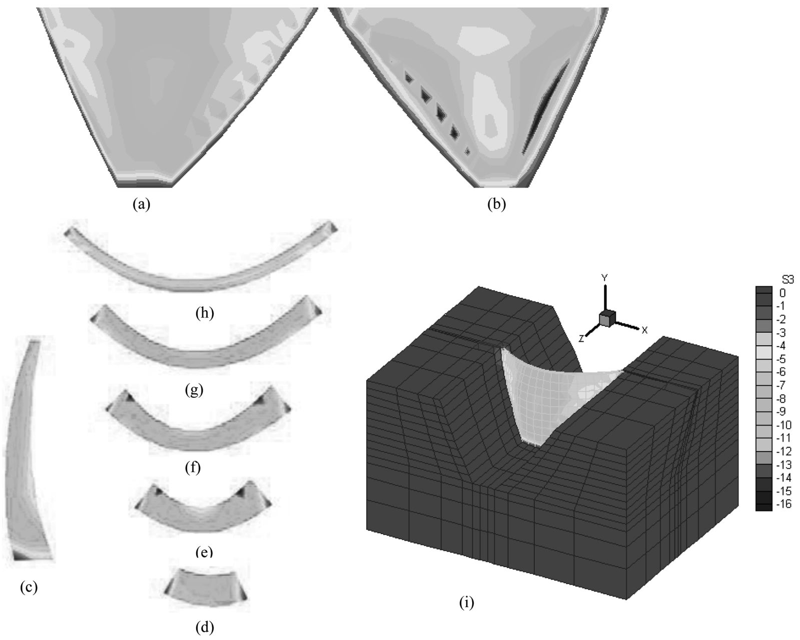

Fig. 18 Principal stress distribution (σ_2) after five years of the dam construction (a) Upstream face, (b) Downstream face, (c) Crown cantilever section, (d) Horizontal section at level = 15 m, (e) Horizontal section at level = 45 m, (f) Horizontal section at level = 75 m, (g) Horizontal section at level = 105 m, (h) Horizontal section at level = 135 m, (i) Block foundation and the dam body

Table 2 Predicted minimum and maximum principal stresses from linear analysis

Stage	σ_1 (MPa)		σ_2 (MPa)		σ_3 (MPa)	
	Min.	Max.	Min.	Max.	Min.	Max.
End of Construction	-5.947	4.924	-7.447	1.065	0.018	-12.24
5 Years After Construction	-6.003	7.942	-7.365	0.739	-0.126	-16.343

Figs. 16-18 show the principal stress distributions after finishing the dam construction by five years. Similar results to that of the end of the dam construction have been observed in locations and distribution shapes. An increase in the tensile and compressive stress values has been noticed. This is due to the cooling of the dam body over the time which normally causes an increase in the stresses especially the tensile one which undesired.

In order to shown the cooling effect of the dam body in the developing of thermal stresses, a comparison has been made between the stresses obtained at the end of construction and those obtained after the dam construction by five years. The value of principle stresses are for the both cases tabulated in Table 2. It is clear from this table that, the increase in the stresses after five years over that obtained immediately at the end of construction is 61.3% for the tensile. that due to the cooling of the dam body with time. The similar observation was also reported by Nilipour (2003).

12. Conclusions

In this investigation an attempt was made to develop two finite element programs, namely

i. Mesh generation finite element program (arch dam-Foundation- bodies system)

ii. Second finite element code was written to predicate arch RCC dam temperature distribution, structural analysis, and combinations of thermal and structural analysis.

Based on the limitations and assumptions used in the present study, the following points can be drawn

- The finite element code developed in this study is capable for simulating the structural response of arch *RCC* dams efficiently. This clearly shown from the reasonable stresses distributions obtained.
- The exposed dam boundaries posses the same air temperature at the end of each stage of analysis. Higher temperature zones are formed at the thicker places near the abutments at lower elevation levels which gradually decreased in values at the upper elevations where the dam thickness correspondingly also decreased. The requirements of strength and crack resistance are greater in high Zone, because of the adiabatic temperature is high in this zone.
- High tensile stresses have been observed at the dam bottom and the abutment boundaries in the upstream side section due to the restriction from the abutment and foundation rock. This is because of low temperature, ranging from dam foundation to abutment and there is no transverse joint in RCC arch dam. Engineers should pay special attention to this zone.
- Compressive stresses contours are concentrated in the dam body in the case of the principal stress σ_1 with high values at the lower part of the upstream face which are gradually decreased in the direction of upper levels and also in the downstream direction.
- Tensile stresses of small values have been observed in the case of the principal stress σ_2 at the

same locations of principal stress σ_1.

- High compressive stress zones concentrated in the upstream side in the case of the principal stress σ_3 which are gradually decreased in the direction of abutment sides and the crest. In addition small regions of high compressive stresses have been observed near the abutment sides.
- An increase in the tensile stresses by 61.3% was observed after five years of dam completion. However the locations and distribution shapes are mostly similar. This attributed to the cooling of the dam body with time, hence post-cooling is not necessary in RCC construction method.

References

ACI 207 1R (1987), "Mass concrete for dams and other massive structures", *ACI Committee*, USA.

ACI 207 5R-99 (2004), "Roller-compacted mass concrete", *ACI Manual of Concrete Practice*, Part 1, USA.

Bayagoob, K.H. (2007), "Thermal and structural analysis of RCC dams", PhD Thesis, Department of Civil Engineering, Universiti Putra Malaysia, Malaysia.

Conrad, M., Aufleger, M. and Malkawi, A.I.H. (2003), "Investigations on the modulus of elasticity of young RCC", *Proceedings of the Fourth International Symposium on RCC Dams*, Madrid, Spain.

Ghanaat, Y. and Clough, R.W. (1989), "EADAP enhanced arch dam analysis program user,s manual, report No. UCB/EERC-89/07", Earthquake Engineering Research Centre, University of California, Berkeley, California.

Xie, H. and Chen, Y. (2005), "Influence of the different pipe cooling scheme on temperature distribution in RCC arch dam", *Commun. Numer. Meth. En.,* **21**, 769-778.

Incropera, F.P. and DeWitt, D.P. (2002), *Fundamentals of Heat and Mass Transfer*, John Wiley & Sons, New York.

Ishikawa, M. (1991), "Thermal stress analysis of a concrete dam", *Comput. Struct.*, **40**(2), 347-352.

Jaafar, M., Bayagoob, K., Noorzaei, J. and Thanoon, W. (2007), "Development of finite element computer code for thermal analysis of roller compacted concrete dams", *J. Adv. Eng. Software*, **38**, 886-895.

Lingfei, X. and Li, Y. (2008), "Research on temperature control and anti-cracking simulation for xiaowan concrete high arch dam", *Proceedings of the International Conference on Computer Science and Software Engineering*.

Nilipour, N. (2003), *Study of Arch Concrete Dams Constructed by RCC Method*, Switzerland, Article in press.

Noorzaei, J., Bayagoob, K., Thanoon, W. and Jaafar, M. (2006), "Thermal and stress analysis of kinta RCC dam", *J. Eng. Struct.*, **28**, 1795-1802.

Noorzaei, J., Thanoon, W.A., Jafaar, M.S. and Zarrini, M.R. (2005), "Modelling of arch dams via finite-infinite-interface elements", *J. Struct. Eng.,* **32**(4), 253-260.

Qiuhua, C. (2003), "New design method of RCC high arch dam", *Proceedings of the Fourth International Symposium on RCC Dams*, Madrid, Spain.

Sergerlind, L.J. (1984), *Applied Finite Element Analysis*, 2nd edition, John Wiley and Sons, New York.

Sheibany, F. and Ghaemian, M. (2006), "Effects of environmental action on thermal stress analysis of Karaj concrete arch dam", *J. Eng. Mech.,* **132**(5), 532-544.

Shuping, H. *et al* (1999), "The emulation analysis of thermal stresses on RCC arch dams", *International Symposium on Roller Compacted Concrete*, China.

Xiaofei. Zhang, Shouyi, L., Yaolong, C. and Junrui, C. (2009), "The development and verification of relocating mesh method for the computation of temperature of RCC dam", *Adv. Eng. Software,* **40**(11), 1119-1123.

Yuksel, S.B. (2009), "Behavior of symmetrically haunched non-prismatic members subjected to temperature changes", *Struct. Eng. Mech.*, **31**(3), 297-314.

Zhang, G.X., Liu, G.T. and Wu, Y. (1996), "Harmonic thermal fracture of multiple crack system and the stability of cracks in RCC arch dam", *Eng. Fract. Mech.,* **54**(5), 653-665.

Zhou, H.F., Ni, Y.Q., Ko, J.M. and Wong, K.Y. (2008), "Modeling of wind and temperature effects on modal frequencies and analysis of relative strength of effect", *Wind Struct.,* **11**(1), 35-50.